Edge Localized Mode Activity as a Limit Cycle in Tokamak Plasmas

Sanae-I. Itoh and Kimitaka Itoh
National Institute for Fusion Science, Nagoya 464-01, Japan

Atsushi Fukuyama
Faculty of Engineering, Okayama University, Okayama 700, Japan

Yukitoshi Miura and JFT-2M Group
Japan Atomic Energy Research Institute, Tokai Ibaraki 319-01, Japan
(Received 9 May 1991)

A model of edge localized modes in tokamak plasmas is presented. A limit-cycle solution is found in the transport equation (time-dependent Ginzburg-Landau type), which has a hysteresis curve for the gradient versus the flux. A periodic oscillation of the particle outflux and an *L*-*H* intermediate state are predicted near the *L*-*H* transition boundary. A mesophase in spatial structure appears near the edge.

PACS numbers: 52.25.Fi, 52.35.Kt

Edge localized modes (ELMs) are a regularly observed phenomenon characterized by the sudden drop of the edge density or temperature with a burst of particles or heat during the *H* phase in tokamak plasmas [1]. When the density or temperature near the plasma edge exceeds a certain threshold value, an *L*- to *H*-mode transition takes place [2]. The ELMs usually follow the *L*-to-*H* transition and show a variety in the magnitude and frequency of the bursts and appear in some restricted parameter space of the *H* phase [1,3–8]. Their experimental characterization has recently begun [3,5]. The *H* mode with small and frequent ELMs is a candidate for standard operation in experimental tokamak reactors. Research to obtain the ELM *y*-*H* mode by an external control (e.g., ELM in the JFT-2M tokamak [7]) is an urgent task. This type of ELM, which we analyze here, has the characteristics that the period and the duration of the burst have similar values, as is shown in Fig. 1, and that it appears near the *L*-*H* transition boundary [7]. There are other ELMs (called "giant ELMs") which are associated with large-amplitude bursts, and appear at some critical pressure near the edge [1,3–8]. Key physical mechanisms for discriminating the various ELMs are not yet known.

To explain the ELMs a comparison with critical-β analysis due to the MHD ballooning mode [3,5] has been applied. The analyses have shown that some ELMs (particularly the small and frequent ones) can occur far below the critical pressure gradient. Resistive MHD analysis [3] of a surface peeling mode may explain some ELMs; however, the assumed current-pressure profiles are not yet experimentally identified. There remains a question for MHD models, since some ELM activities are insensitive to the q value. Namely, the observed soft-x-ray emission profiles of ELMs do not shift when the surface q value is varied from 2.4 to 5.6 [2]. Therefore ELMs are not considered to be located at a certain rational surface. The period and duration of small and frequent ELMs are left unsolved in the MHD analysis.

A model of ELMs as a cyclic oscillation between *L* and *H* phases due to impurity accumulation has been proposed [9]. Up to now, however, the impurity accumulation has been considered to be an associated phenomenon [3,10].

In this paper we propose a more complete model of small and frequent ELMs, shown in Fig. 1. The *L*-*H* transition has been observed to yield a hysteresis curve for the thermodynamic forces (e.g., the density/temperature gradients) versus the associated flows [2,3]. Previous theories [11,12] have predicted a sudden change in loss flux through the radial electric field (E_r) bifurcation [11] and the poloidal flow bifurcation [12] near the edge. Two models predicted a hysteresis curve for flux versus gradient, but with a different change in the sign of E_r for given boundary conditions.

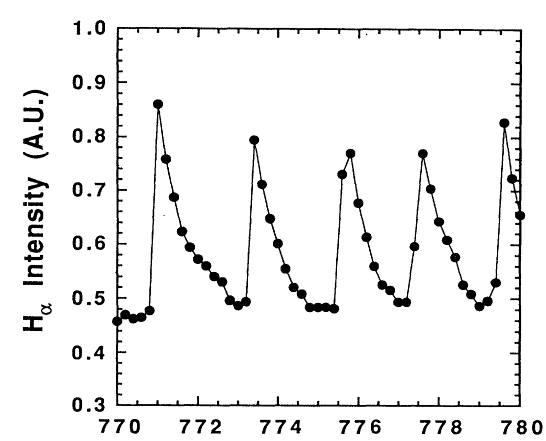

FIG. 1. Time trace of the H_α intensity of the "grassy" *H* mode in the JFT-2M tokamak. H_α is given in arbitrary units. For details of the discharge conditions, see Ref. [7].

Motivated by the theories, experimental checks have been done. It was observed in D-III-D [13] that poloidal flow changes significantly and E_r jumps to a more negative value. Further E_r profile measurements on JFT-2M [14] confirmed the E_r change and revealed that dE_r/dr becomes more negative. Active biasing experiments on CCT [15] and TEXTOR [16] have shown that the *L-H* transition can be induced by both positive and negative biasing. From these researches it is understood that the *L-H* transition involves sudden changes of both dE_r/dr and the sheared poloidal flow. Regardless of the sign of E_r, a picture of the bifurcation between multiple states is supported. (Theoretically, the sign of E_r depends on the boundary conditions imposed on the plasma.) However, quantitative tests of the models on the threshold condition and the transport barrier are not complete; the spatial-temporal structure was not analyzed theoretically and the thickness of the barrier was introduced as a parameter in the theories. Also awaiting investigation is whether the physics picture of Refs. [11,12] can predict the dynamics of ELMs which are also characteristics of the *H* mode.

The theories of Refs. [11,12] are extended to include the temporal evolution and the spatial diffusion. The newly obtained equations for the edge density and E_r (or V_θ) are of the time-dependent Ginzburg-Landau type [17], which contain the solution of a limit-cycle oscillation. This oscillation is attributed to be one class of small and frequent ELMs. A model S curve is employed for the phase diagram of the density gradient and the particle flux. The radial structure is obtained and it shows the existence of an intermediate phase (mesophase) of the diffusivity between the *L* and the *H* phases near the edge region. We assume a uniform temperature, since the ELMs of interest here are experimentally insensitive to the heating power.

The model equations consist of the radial transport equations for the density n, with the effective diffusivity D, and for the normalized radial electric field (or poloidal rotation) Z, with the viscous diffusivity μ. The value of D can be multivalued and is a function of Z. The equations are given by

$$\frac{\partial n}{\partial t}=\frac{\partial}{\partial x}D(Z)\frac{\partial n}{\partial x}\,, \tag{1}$$

$$\varepsilon\frac{\partial Z}{\partial t}=-N(Z,g)+\mu\frac{\partial^2 Z}{\partial x^2}\,. \tag{2}$$

The parameter ε is a small coefficient showing that Eq. (2) has a faster time scale than Eq. (1) when μ and D have similar magnitudes. The nonlinear term N corresponds to the radial current $\Gamma_e-\Gamma_i$ in local theory (i.e., shear viscosity is neglected), which arises from ion orbit loss, drift wave convection, and ion parallel viscous damping [11,12]. The existence of multiple states was predicted by solving the local net-current-free condition, $N(Z,g)=0$, to obtain $Z(g)$. The variable g corresponds to $d\lambda$, where $\lambda=\rho_p n'/n$, $d=D_0/\nu\rho_p^2$, ρ_p is the ion poloidal gyroradius, ν is the ion collisionality, and D_0 is a typical electron diffusivity. Contrary to the local theory in which $N(Z,g)=0$ is solved, here $Z(x,t)$ is calculated and the evolution of $D(x,t)$ is obtained. We use the model S curve for N, and D is assumed to be a smooth function of Z,

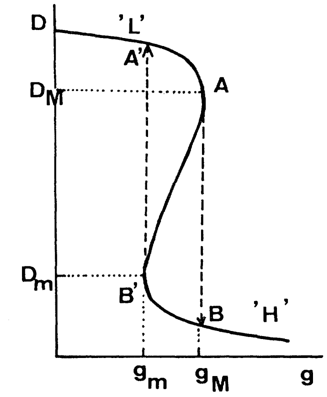

FIG. 2. Model of effective diffusivity D (i.e., ratio of the particle flux to the density gradient) as a function of gradient parameter g. See text for the definition and normalization. ($\alpha=1$, $\beta=1$, $D_{\rm max}=3$, $D_{\rm min}=0.01$, $g_0=1$.)

$$N(Z,g)=g-g_0+[\beta Z^3-\alpha Z]\,,$$

$$D(Z)=\tfrac{1}{2}(D_{\rm max}+D_{\rm min})+\tfrac{1}{2}(D_{\rm max}-D_{\rm min})\tanh Z\,.$$

In writing explicit forms for N and D, we normalize x by ρ_p, D and μ by D_0, t by ρ_p^2/D_0, and flux Γ by $D_0 n_0/\rho_p$. μ/D_0 is the diffusion Prandtl number P_D. The normalizing density n_0 is chosen so as to satisfy $g_0=1$. $\varepsilon\simeq(\rho/\rho_p)^2$ (ρ is the ion gyroradius) and $\varepsilon\ll 1$ [18]. The parameters g_0, α, β, $D_{\rm max}$, $D_{\rm min}$, and μ/D_0 are treated as constants. A typical curve of $D(g)$ for $N(Z,g)=0$ is shown in Fig. 2. The large-D and the small-D branches correspond to the *L* and the *H* states, respectively.

We numerically solve Eqs. (1) and (2), with the simple condition that $\partial Z/\partial t=0$ (i.e., $\varepsilon=0$). Equation (2) is a kind of time-dependent Ginzburg-Landau equation [17], the one which is used to analyze the reaction diffusion system in chemical reactions. The system contains a so-called slow manifold structure due to the assumption $\varepsilon\ll 1$.

The slab region near the plasma edge, $-L<x<0$, is our interest. For the boundary conditions at the plasma edge ($x=0$), we impose the constraint that $(n'/n)^a n^b$ is fixed. A simulation analysis on the scrape-off-layer plasma transport has shown that $|b/a|\ll 1$ holds [19], and we discuss here the case of $a=1$ and $b=0$. At the core side ($x=-L$), we give the particle flux $\Gamma_{\rm in}$.

Solving Eqs. (1) and (2) with $\varepsilon=0$ we find a state with periodic oscillations of the edge density n_s and of the loss flux $\Gamma_{\rm out}$ in a restricted parameter space near the boundary of the *L* and *H* states. The flux $\Gamma_{\rm out}$ is defined at

$x=0$. In Fig. 3, the temporal evolution of Γ_{out}, which corresponds to the H_α burst, and the Lissajous figure for n_s and Γ_{out} are shown. The parameters are $g_0=1$, $\alpha=0.2$, $\beta=0.2$, $D_{max}=3$, $D_{min}=0.01$, $\mu=1$, $\Gamma_{in}=3$, and λ_s ($\equiv -n/n'$ at the edge) $=1.25$.

These oscillating solutions are attributed to the ELM y-H mode. The parameter space where the ELM y-H mode appears is found to be

$$D_m/g_m < \Gamma_{in}\lambda_s^2 < D_M/g_M\,, \tag{3}$$

where $g_m=g_0-2\beta(\alpha/3\beta)^{3/2}$, $g_M=g_0+2\beta(\alpha/3\beta)^{3/2}$, $D_m=D(Z=\sqrt{\alpha/3\beta})$, and $D_M=D(Z=-\sqrt{\alpha/3\beta})$, as shown in Fig. 2. In this parameter regime, a limit-cycle solution on the D-g plane (at the edge) appears. When Γ_{in} is large enough to satisfy $\Gamma_{in}\lambda_s^2 > D_M/g_M$, we find the stationary L state; the H state with steep density gradient is found in the region $\Gamma_{in}\lambda_s^2 < D_m/g_m$. If $D_m/g_m > D_M/g_M$ holds, no oscillation is allowed. Details will be reported elsewhere [20].

In Figs. 3(c) and 3(d), the radial structures of the density and the effective diffusion coefficient D are shown at the times of high and low confinement. A transport barrier near the edge, at which D is reduced, is formed in a phase of rising density. A smooth curve for D is formed due to the finite viscosity μ [21]. The spatial structure of D shows the existence of a mesophase of the L and H phases near the edge. (In the mesophase, D has a value intermediate between those for the H and L branches in Fig. 2.) The thickness Δ is estimated as $\Delta\simeq\sqrt{2\beta\mu/\alpha}$ in the small-μ limit. A numerical calculation gives $\Delta \propto \mu^{0.44}$, confirming this analysis. (L satisfies $L\gg\Delta$, so

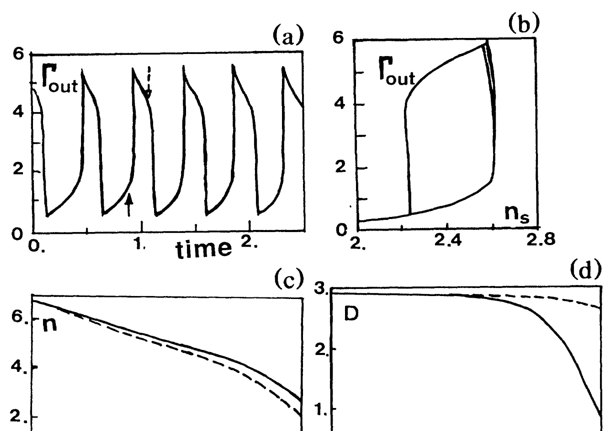

FIG. 3. (a) Temporal evolution of the outflux and (b) the Lissajous figure for the edge density and the outflux. Parameters are $\alpha=0.2$, $\beta=0.2$, $\mu=1$, $\Gamma_{in}=3$, $\lambda_s=1.25$, and others are the same as in Fig. 2. Spatial profiles of (c) density and (d) diffusivity. The time slice is denoted by arrows in (a). The solid and dashed lines are for before the burst and at the end of the burst, respectively.

that Δ is not limited by the computation region.) In this region, poloidal rotation exists. The width Δ is different from the width of the density inversion region.

We study the parameter dependence of the period τ of the oscillation. The numerical computation gives $\tau \simeq C\alpha\lambda_s\Delta D_M^{-1}$, where C is a numerical coefficient of the order of unity. As is shown in Eq. (3), λ_s is bounded in a narrow region for realization of the oscillation. If the ratio λ_s^2/D_M and other parameters are fixed, we have $\tau\propto D_M^{-0.5}$ over a wide range. On the other hand, if the value of $\Gamma_{in}\lambda_s^2$ and other parameters are fixed, we have $\tau\propto\Gamma_{in}^{-0.5}$.

The ratio of the time interval of good confinement (τ_H) to τ, $\eta=\tau_H/\tau$, represents how close the intermediate state is to the H mode. (In the H mode, $\eta=1$; $\eta=0$ for the L mode.) In the parameter space predicted by Eq. (3), η takes intermediate values between 1 and 0. η is a decreasing function of $\Gamma_{in}\lambda_s^2$, and is discontinuous at the boundaries D_m/g_m and D_M/g_M. For oscillating solutions, η takes its largest value η_{max} at $\Gamma_{in}\lambda_s^2=D_m/g_m$. η_{max} increases and approaches unity if D_m becomes close to D_{min}. This is confirmed by reducing D_m to D_{min} by fixing g_m. For instance, by taking $\alpha=0.2$ and $\beta=\alpha^3$, η can be greater than 0.95, i.e., the period is 20 times longer than the pulse width. In other words, the degree of H mode depends on the transition structure.

In summary, a theoretical model of ELMs is developed by extending the bifurcation model to the time-dependent diffusive media. A time-dependent Ginzburg-Landau model equation with the spatial diffusion is applied. A periodic solution of the plasma density and outflux is found, revealing a sequence of bursts of plasma loss. This model reproduces the oscillations in which the decay time of the loss and the period are comparable. The region of this nonlinear oscillation is identified to be near the L-H modes boundary. The degree of H mode, η, which represents the L-H intermediate state, is studied. The parameter dependence of the period is studied. A mesophase of the diffusivity between the L and H phases is found near the plasma boundary. The width of the transport barrier was found to be proportional to $(\beta P_D/\alpha)^{1/2}$. The importance of the ion viscosity on the pedestal is shown. The interpretation of the parameters (α,β,D_m,D_M) in terms of physical quantities depends on bifurcation models. A simple extension from Ref. [11] gives $\alpha=3\beta\simeq3[1-d\sqrt{\ln(2e/d)}]/2[1+d\sqrt{\ln(2e/d)}]$, $D_M\simeq d$, and $D_m\simeq d/2(\ln 2e/d)$. For fixed Γ_{in} and λ_s, the value of d delimits the regions of the L, ELM y-H, and H modes. These relations provide a test for comparison when experimental measurements of the shear viscosity near the edge is made. For the case of $\varepsilon\neq0$, a similar result is reproduced when ε is small ($\varepsilon\lesssim0.5$ for the case of Fig. 1). Fluctuations in the source or external oscillations cause chaotic oscillations of n, Γ_{out}, and E_r. The interpretation of Eq. (3) for various models and the following study requires further effort; some will be given in Ref. [20].

This work is partly supported by a Grant-in-Aid for

Scientific Research of the MoE, Japan, and by the collaboration program between universities and JAERI on fusion. The authors thank Professor A. Lichtenberg for discussion and a critical reading of the manuscript.

[1] M. Keilhacker *et al.*, Plasma Phys. Controlled Fusion **26**, 49 (1984).
[2] F. Wagner *et al.*, Phys. Rev. Lett. **49**, 1408 (1982).
[3] ASDEX Team, Nucl. Fusion **29**, 1959 (1989).
[4] P. Gohil *et al.*, Phys. Rev. Lett. **61**, 1603 (1988); D. H. Hill *et al.*, Nucl. Fusion **28**, 902 (1988); D. P. Schissel *et al.*, Nucl. Fusion **29**, 185 (1989).
[5] DIII-D Team, in *Proceedings of the Thirteenth International Conference on Plasma Physics and Controlled Nuclear Fusion Research, 1990, Washington, DC* (IAEA, Vienna, 1991), paper No. CN-53/A-1-4.
[6] T. Shoji *et al.*, in *Proceedings of the Seventeenth European Conference on Controlled Fusion and Plasma Physics, Amsterdam, 1990* (European Physical Society, Amsterdam, 1990), Pt. 3, p. 1452.
[7] Y. Miura *et al.*, in *Proceedings of the Thirteenth International Conference on Plasma Physics and Controlled Nuclear Fusion Research* (Ref. [5]), paper No. CN-53/A-4-6.
[8] T. Osborne *et al.*, Bull. Am. Phys. Soc. **35** (9), 1975 (1990).
[9] T. Ohkawa, S.-I. Itoh, and K. Itoh, Kaku Yugo Kenkyu **59**, 488 (1988).
[10] F. Wagner *et al.*, in *Proceedings of the Thirteenth International Conference on Plasma Physics and Controlled Nuclear Fusion Research* (Ref. [5]), paper No. CN-53/A-4-2.
[11] S.-I. Itoh and K. Itoh, Phys. Rev. Lett. **60**, 2276 (1988); J. Phys. Soc. Jpn. **59**, 3815 (1990).
[12] K. C. Shaing and E. C. Crume, Phys. Rev. Lett. **63**, 2369 (1989).
[13] R. J. Groebner, K. H. Burrell, and R. P. Seraydarian, Phys. Rev. Lett. **64**, 3015 (1990).
[14] K. Ida, S. Hidekuma, Y. Miura, T. Fujita, M. Mori, K. Hoshino, N. Suzuki, T. Yamauchi, and JFT-2M Group, Phys. Rev. Lett. **65**, 1364 (1990).
[15] R. J. Taylor, M. L. Brown, B. D. Fried, H. Grote, J. R. Liberati, G. J. Morales, P. Pribyl, D. Darrow, and M. Ono, Phys. Rev. Lett. **63**, 2365 (1989).
[16] R. R. Weynants *et al.*, in *Proceedings of the Thirteenth International Conference on Plasma Physics and Controlled Nuclear Fusion Research* (Ref. [5]), paper No. CN-53/A-6-6.
[17] E. M. Lifshitz and L. P. Pitaevskii, *Statistical Physics Part 2,* Landau and Lifshitz Course of Theoretical Physics Vol. 9 (Pergamon, Oxford, 1980), Sec. 45.
[18] S.-I. Itoh and K. Itoh, Nucl. Fusion **29**, 1031 (1989).
[19] S.-I. Itoh, N. Ueda, and K. Itoh, Plasma Phys. Controlled Fusion **32**, 415 (1990).
[20] S.-I. Itoh, K. Itoh, and A. Fukuyama, NIFS Report No. 96 (to be published).
[21] E. Yahagi, K. Itoh, and M. Wakatani, Plasma Phys. Controlled Fusion **30**, 995 (1988).